PROCEEDINGS, 49th Workshop on Geothermal Reservoir Engineering
Stanford University, Stanford, California, February 12-14, 2024
SGP-TR-227

Summary of Annual Repeat Magnetotelluric Surveys of the Geysers Geothermal Field

Jared R. Peacock[1], David L. Alumbaugh[2], Michael A. Mitchell[1], Craig Hartline[3]

[1]U.S. Geological Survey, P.O. Box 158, Moffett Field, CA 94035, USA

[2]Lawrence Berkeley National Lab, 1 Cyclotron Road Mail Stop 74-316C Berkeley, CA 94720, USA

[3]Calpine Corporation, 10350 Socrates Mine Rd, Middletown, CA 95461, USA

jpeacock@usgs.gov

Keywords: Magnetotellurics, monitoring, The Geysers, repeat measurements, three-dimensional modeling

ABSTRACT

As part of a multi-year project, funded by the California Energy Commission, annual magnetotelluric (MT) surveys have been collected at The Geysers geothermal field in northern California with the goal of measuring temporal changes within the steam field. The repeat surveys started in 2021 and repeated a 2017 survey (Peacock et al., 2020) with further extension to the southern part of the geothermal field. Temporal variations in the MT transfer functions are observed to be spatially coherent and compartmentalized. Mapping residual phase tensor ellipses demonstrates the direction of maximum change is often aligned with existing fracture orientations. Three-dimensional inversion of the MT data, using the inversion results from previous years as the starting model, indicates that the steam reservoir has generally become more resistive over time (~10%), suggesting more steam in the field. A few pockets within the steam field have become more electrically conductive over time and are collocated with injection wells, suggesting either more fluid content in those zones, less steam, or more saline fluids.

1. INTRODUCTION

The Geysers geothermal reservoir in northern California is the world's largest energy producing geothermal steam field. The field has been producing geothermal energy for over 60 years, resulting in significant changes to the reservoir. Production declined in the 1980's due to pressure loss from steam extraction without replenishment (Stark et al., 2005). Reinjection projects using treated wastewater from nearby municipalities were developed to increase steam production, including the 1997 Southeast Geysers Effluent Pipeline (Brauner & Carlson, 2002), and the 2003 Santa Rosa Geysers Recharge Project (SRGRP) (Stark et al., 2005). Over time production has stabilized; however, injection has incresed the complexity of fluid flow patterns within the vapor-dominated field. In 2010, Calpine began development of an enhanced geothermal system (EGS) demonstration project in the Northwest Geysers (Garcia et al., 2016). The EGS stimulates a deep (>3 km) high-temperature reservoir, with measured temperatures up to 400 °C, using treated wastewater from the SRGRP (Garcia et al., 2016).

To help understand temporal subsurface variations, the California Energy Commission funded a multi-year project led by Lawerence Berkeley National Lab to monitor The Geysers geothermal field using constant passive seismic measurements coupled with annual MT surveys. The project began in 2020 and will conclude in mid-2024. The end product will be a set of joint inversions of electrical resistivity and seismic velocity at three different points in time using a cross-gradient method (Um et al., 2014, Um et al., 2023). Presented here is a brief summary of the repeated MT measurements including residual phase tensor analysis and preliminary 3D modeling.

2. MAGNETOTELLURIC DATA

In July of 2017, an MT survey comprised of 42 stations was collected at The Geysers (Peacock et al., 2020a), which focused mainly on the northern part of the geothermal field (Figure 1). These data were used to develop a 3D electrical resistivity model detailed in Peacock et al. (2020b). For this project, the original 42 stations were are repeated along with 13 new stations in the southern part of the field (Figure 1). Phase 1 was collected in April of 2021 (Peacock et al., 2022), Phase 2 was collected in April of 2022 (Peacock et al., 2023), and Phase 3 was collected in April of 2023.

When possible, MT data were collected at the same locations with the same data loggers, magnetic sensors, and electrodes to reduce measurement error. Each MT station included two horizontal orthogonal ANT-4 magnetic induction coils (Zonge International, Tucson, Arizon) and two orthogonal electrical dipoles with a nominal length of 50 m, dependent on vegetation and topography. Electric potentials were measured with Ag-AgCl Stelth 1 solid-state electrodes (Borin Manufacturing, Culver City, California) placed in a saturated canvas bag of bentonite clay to reduce contact resistance and buried a few inches below the surface. Typical contact resistances are between ~1–7 kOhm. Each MT station was oriented with respect to geomagnetic north using a Brunton compass and sighting compass for the electric dipoles. All four components were connected to a 5-channel 32-bit ZEN data logger manufactured (Zonge International, Tucson, Arizona). The data were recorded on a repeating schedule of 5 hours and 50 minutes sampling at 256 samples/second, and 10-minutes sampling at 4,096 samples/second. The schedules were set such that all active instruments recorded the sampling rates synchronously to allow for remote reference processing.

To estimate the MT transfer functions, two processing codes were used. The data were first processed using the bounded-influence robust remote reference code *BIRRP* (Chave and Thomson, 2004). *BIRRP* allows for multiple remote references, where synchronous local stations are used to identify and remove incoherent noise between the stations, which is important in a noisy environment like The Geysers. Each station takes between 15-30 minutes to process depending on input data and program settings. The same processing parameters are used for each repeated station to remove bias caused by algorithm parameters. This provides transfer function estimates for frequencies from 1,000 Hz to 0.25 Hz. To estimate longer periods the open-source Python processing code *Aurora* (Kappler et al., 2024) was employed. Magnetic observatory data from Fresno (350 km southeast of the study area) were used as a distant remote reference (Kerridge, 2001). All MT data collected at a single station are down sampled to 1 sample per second and combined into a single time series to be processed with the magnetic observatory data to estimate MT transfer functions between 0.25 Hz to 0.001 Hz. This processing reduces bias from local noise sources and low signal in the natural MT dead band (1 to 0.05 Hz). The output transfer functions from *BIRRP* and *Aurora* are then combined to produce an MT transfer function that spans the frequency range of 1,000 Hz to 0.001 Hz. Given the amount of infrastructure and cultural noise at The Geysers, the MT transfer functions are of good quality (Peacock et al., 2022).

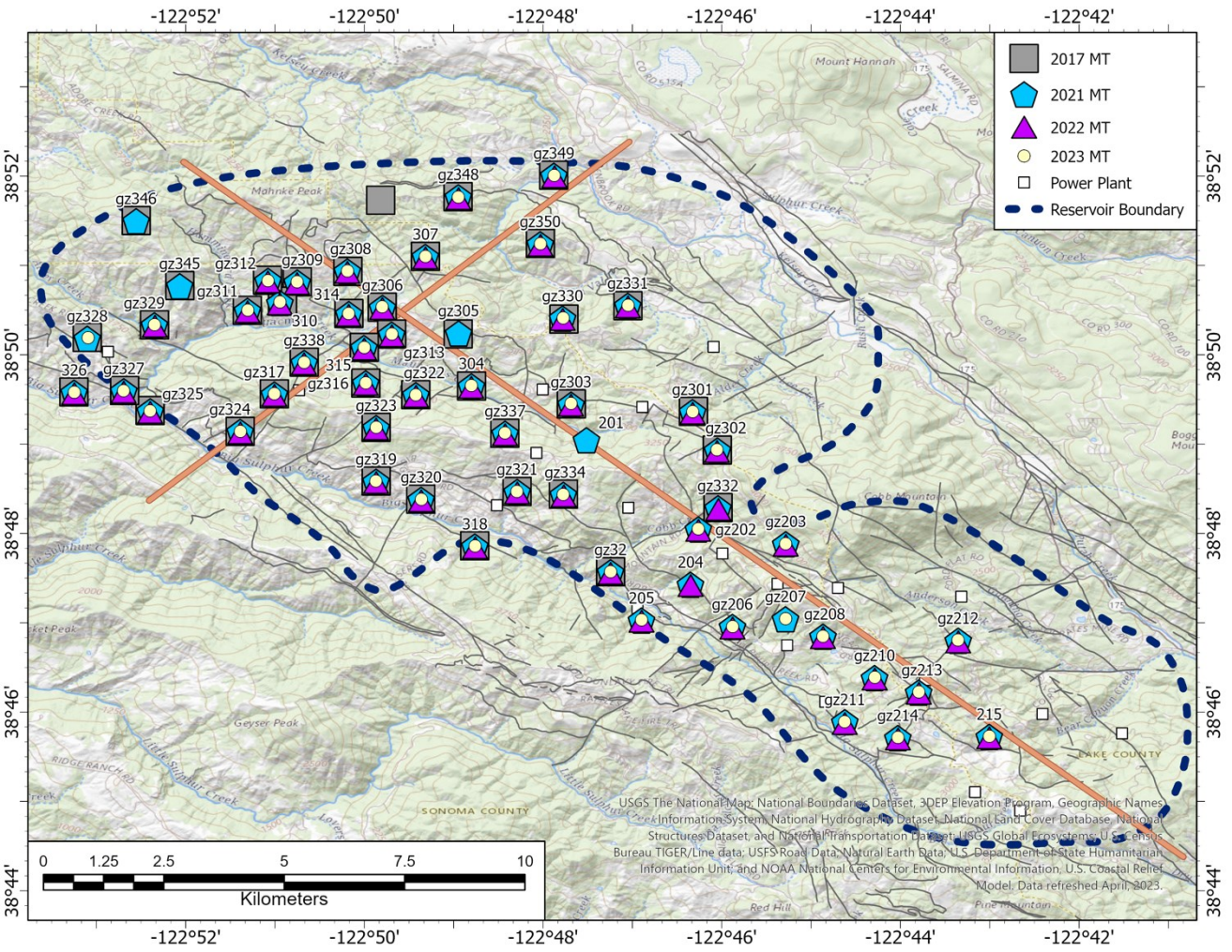

Figure 1: Map of repeated MT stations collected to monitor The Geysers geothermal field. Gray squares: MT stations collected in 2017; blue pentagons: Phase 1 MT stations collected in 2021; magenta triangles: Phase 2 MT stations collected in 2022; yellow circles: Phase 3 MT stations collected in 2023; white squares: operating power plants; dotted line: estimated boundary of the steam reservoir; orange lines: profiles shown in subsequent figures; gray lines: mapped faults. Base map is from the U.S. Geological Survey National Map (U.S. Geological Survey, 2020). Map image is the intellectual property of Esri and is used herein under license. Copyright © 2020 Esri and its licensors. All rights reserved.

3. PHASE TENSOR ANALYSIS

MT transfer functions can be represented using the phase tensor (Caldwell et al., 2004), which is a distortion-free, rank 2, frequency-dependent tensor. Invariants of the phase tensor provide directional information as well as information about whether the subsurface is becoming more resistive or conductive (Caldwell et al., 2004). One way of comparing two MT data sets is to calculate the residual phase tensor (Peacock et al., 2012). The residual phase tensor is also invariant to near-surface distortions and provides directional information about how the subsurface changes between two MT transfer functions but does not indicate whether the subsurface is becoming more resistive or conductive. Graphically the residual phase tensor is represented by an ellipse (Figure 2 and 3). Ellipse elongation indicates a

larger resistivity change in the direction of the long axis. The color of the ellipse represents the percent change between transfer functions but does not indicate if the change was more resistive or more conductive.

In general, changes are on the order of 5-20% between surveys except between 2022 and 2023 when changes were generally smaller, suggesting little change over the period of one year. In map view, the residual phase tensor indicates compartmentalized changes of subsurface resistivity variations within the steam field (Figure 2). The orientation of these residual phase tensor ellipses could be related to fault orientation, fluid injection, or temporal changes in fluid flow within preexisting fault structures.

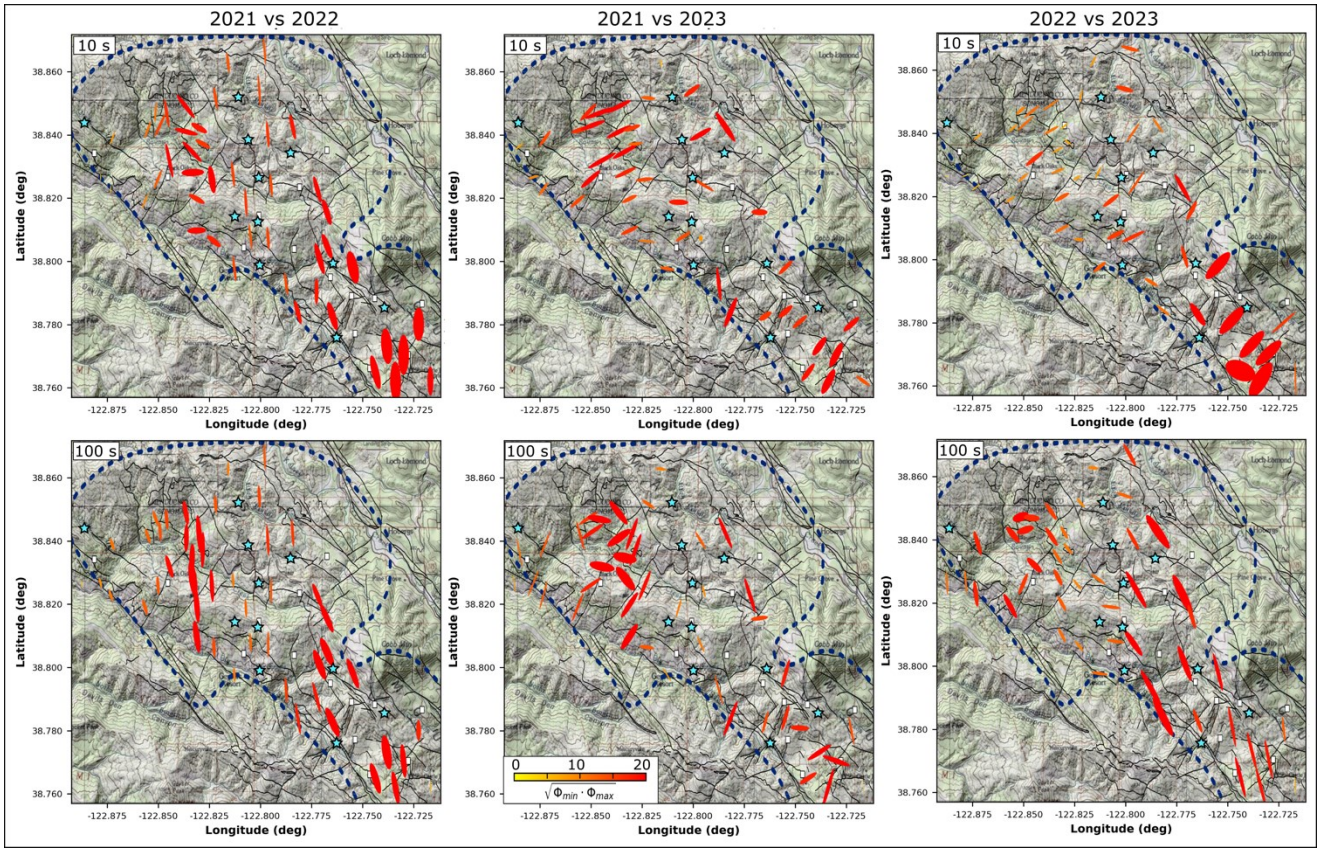

Figure 2: Example of residual phase tensor ellipses plotted in map view on top of a topographic map. The title of each column represents the survey years for which the residual phase tensors are computed. The top row and bottom rows show residual phase tensors for periods of 10 seconds (~ 1 km depth) and 100 seconds (~5 km depth), respectively. The color map is the same for each plot and represents the percent change between surveys. Dark blue dashed line: general outline of the geothermal field; white squares: active power plants; cyan stars: injection wells; gray lines: mapped faults. Ellipse orientations are aligned with the direction of maximum change. Changes are compartmentalized within the geothermal field possibly related to fluid injection, and the changes from 2022 to 2023 are smaller than for the other two periods. The residual phase tensor does not contain information about whether the changes represent a reduction or increase in resistivity. Base map is from the U.S. Geological Survey National Map (U.S. Geological Survey, 2020). The map image is the intellectual property of Esri and is used herein under license. Copyright © 2020 Esri and its licensors. All rights reserved.

In a cross-section view, also known as a pseudo section, changes in the residual phase tensors are confined to a certain period range (2 to 1000 seconds) and are again compartmentalized (Figure 3). Here residual phase tensor ellipses are plotted versus period. Period is a proxy for depth and is related to the bulk apparent resistivity, where longer periods are related to deeper structures. At The Geysers, residual phase tensors with a period of 2 seconds are sensitive to conductivity variation at approximately 1 km depth. Figure 3 shows two pseudo sections for each year-to-year comparison: along a northeast profile (top) and a northwest profile (bottom) defined in Figure 1. The northeast profile indicates that subsurface changes occur to the west of an injection, similarly the northwest profile suggests changes occur to the northwest of an injection well. Both suggesting more permeability to the west and north of the injection well (Peacock et al., 2020). The southern end of the northwest profile is noisier and shows more erratic orientations and shapes among the residual phase tensors.

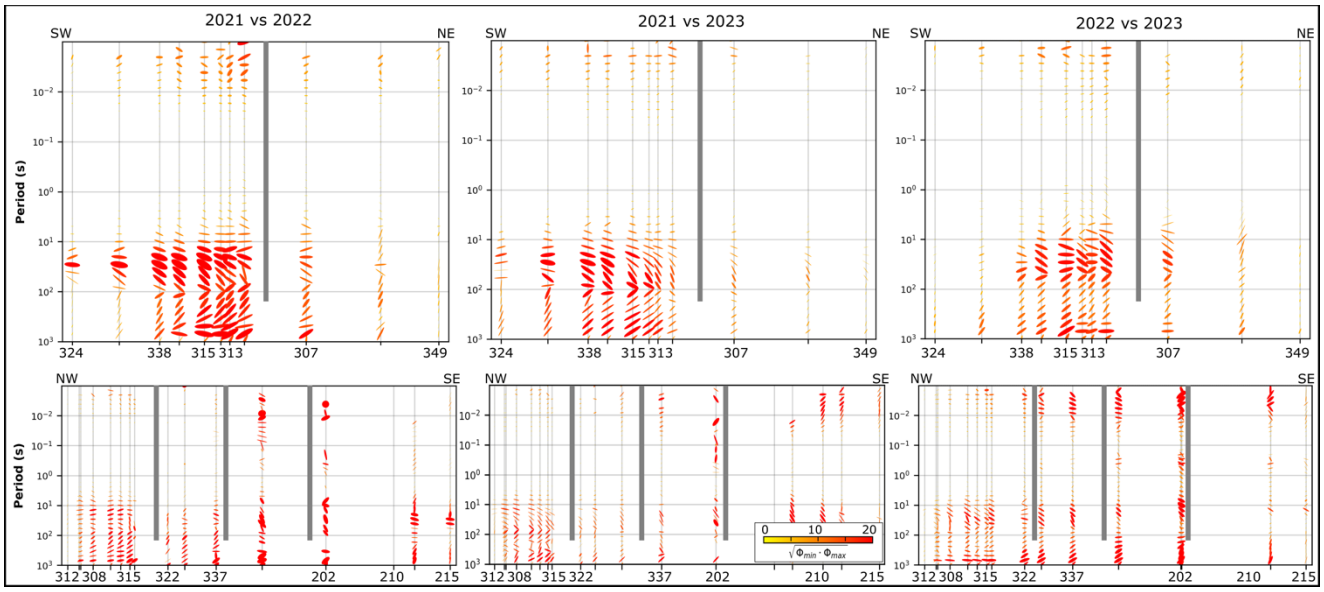

Figure 3: Residual phase tensor pseudo sections for the profile lines in Figure 1. Each column title describes the surveys compared. Ellipses are plotted as a function of period, which is a proxy for depth. Ellipse orientation is in map view where North is up and East is to the right. Each plot uses the same color scale. Gray lines show the approximate locations of injection wells. Note that in the northeast-southwest profile (top row) the asymmetry in changes relative to the injection well suggests enhanced permeability to the west of the injection well. The ellipses at the southern end of the northwest-southeast profile are noisy making interpretations of subsurface changes difficult.

4. MODELING

To image subsurface changes observed in the MT response and residual phase tensors, 3D modeling is needed. The 3D inverse modeling was completed using ModEM (Egbert et al., 2012, Kelbert et al., 2014) on the U.S. Geological Survey high-performance computer Yeti (Falgout and Gordon, 2018). Data for each survey were interpolated onto the same period range (500 Hz – .001 Hz) and edited for obvious outliers. The model mesh includes topography and has dimensions of 95 x 115 x 80 cells (300 x 300 x 200 km) with cell sizes of 200 x 200 m within the station area. Cell thickness starts at 30 m and increases to 200 m thickness at 5 km depth, to match the seismic tomographic model grid of Gritto et al., 2022, and then increases geometrically downwards to account for edge effects. Normalized root-mean-squared errors were around 1.6 for all surveys using an error floor of 3%. The resulting model from the 2021 survey (Peacock et al., 2022) was used as the starting model for inverting the 2022 and 2023 data separately. The resulting 2022 model (Peacock et al., 2023) was also used as a starting model for inverting the 2023 data. The models between the surveys were subsequently subtracted to estimate subsurface changes between surveys. Figure 4 show an example of the difference between the 2021 and 2022 electrical resistivity models indicating that subsurface changes are compartmentalized and possibly related to fluid injection. The 2023 model is not shown as results are still preliminary.

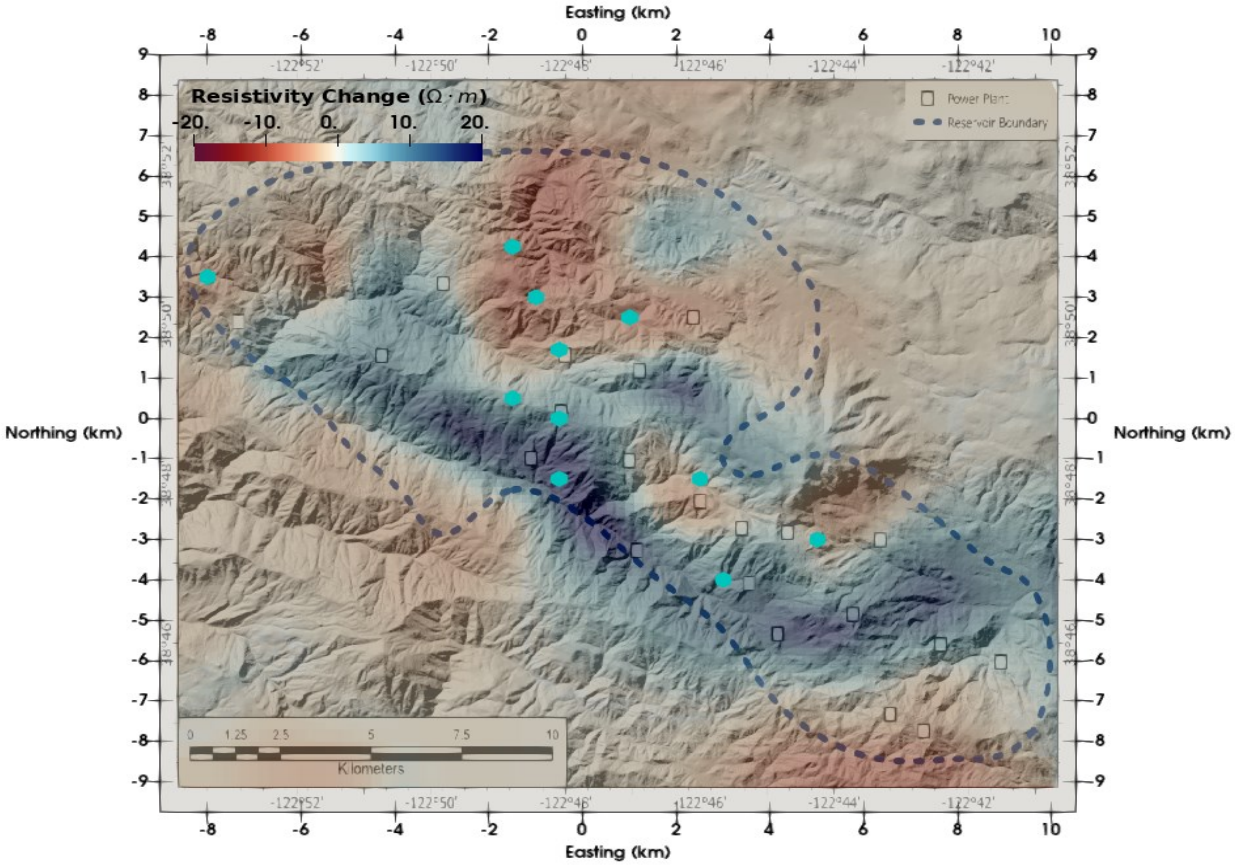

Figure 4: Example of temporal differences between the 2021 and 2022 3D electrical resistivity models for a horizontal slice at 1 km depth plotted on top of a topographic map Base map is from the U.S. Geological Survey National Map (U.S. Geological Survey, 2020). Cyan hexagons mark the approximate locations of injection wells. Blue colors indicate that the subsurface has become more resistive over time, whereas red colors indicate an increase in conductivity over time. Resistivity changes are compartmentalized and often associated with injection wells.

5. CONCLUSIONS

Repeat MT measurements have been successfully collected at The Geysers over the course of three years. Comparing the MT response and residual phase tensors suggests subsurface changes are compartmentalized and likely related to fluid injection and existing fault structures. Inverting each survey in 3D using a prior survey as a starting model supports initial observations of the MT response and residual phase tensors highlighting regions that became more or less resistive over time. Those regions that became less resistive over time could indicate an increase in the fluid content, whereas those that became more resistive likely indicates an increase in the steam content. To further understand subsurface resistivity changes other geophysical information could be incorporated into the model. A joint inversion with contemporaneous passive seismic data (Gritto et al., 2022) using a cross-gradient method (Um et al., 2014) would yield a more comprehensive 3D geophysical model (Um et al., 2023), from which physical properties important to steam production could be interpreted.

Note: Any use of trade, firm, or product names is for descriptive purposes only and does not imply endorsement by the U.S. Government.

REFERENCES

Brauner, E., & Carlson, D. C. (2002). *Santa Rosa Geysers Recharge Project: GEO-98-001.* California Energy Commission. Office of Scientific and Technical Information (OSTI). https://doi.org/10.2172/897791.

Caldwell, T. G., Bibby, H. M., & Brown, C. (2004). The magnetotelluric phase tensor. *Geophysical Journal International, 158*, 457–469. https://doi.org/10.1111/j.1365-246x.2004.02281.x.

Chave, A. D., & Thomson, D. J. (2004). Bounded influence magnetotelluric response function estimation. *Geophysical Journal International, 157*, 988-1006. https://doi.org/10.1111/j.1365-246X.2004.02203.x.

Egbert, G. D., & Kelbert, A. (2012). Computational recipes for electromagnetic inverse problems. *Geophysical Journal International, 189*, 251–267. https://doi.org/10.1111/j.1365-246X.2011.05347.x.

Garcia, J., Hartline, C., Walters, M., Wright, M., Rutqvist, J., Dobson, P. F., & Jeanne, P. (2016). The Northwest Geysers EGS Demonstration Project, California. *Geothermics, 63*, 97–119. https://doi.org/10.1016/j.geothermics.2015.08.003.

Gritto, R., Jarpe, S. P., & Alumbaugh, D. L. (2022). New large-scale passive seismic monitoring at The Geysers geothermal reservoir, CA, USA. *Proceedings, 47th Workshop on Geothermal Reservoir Engineering*, Stanford University, Stanford, CA, 1-11.

Falgout, Jeff T, Janice Gordon, (2018). USGS Advanced Research Computing, USGS Yeti Supercomputer: U.S. Geological Survey, https://doi.org/10.5066/F7D798MJ.

Kappler, K., Peacock, J. R., Capriotti, J., Heagy, L., Ronan, T., Kang, S. (2024) Aurora v0.3.12, Zenodo, https://doi.org/10.5281/zenodo.10494538.

Kelbert, A., Meqbel, N. M., Egbert, G. D., & Tandon, K. (2014). ModEM: a modular system for inversion of electromagnetic geophysical data. *Computers & Geoscience, 66*, 40–53. https://doi.org/10.1016/j.cageo.2014.01.010.

Kerridge, D. J. (2001), INTERMAGNET: World-wide near-real-time geomagnetic observatory data, paper presented at Space Weather Workshop: Looking Towards a European Space Weather Programme, Eur. Space Res. and Technol. Cent., Noordwijk, Netherlands, 17–19 Dec.

Peacock, J. R., Alumbaugh, A., Mitchell, M. A., Hartline, C., (2022). Repeat magnetotelluric measurements to monitor The Geysers steam field in northern California, *47th Workshop on Geothermal Reservoir Engineering*, *SGP-TR-233,* Stanford, California.

Peacock, J. R., Alumbaugh, A., Mitchell, M. A., Hartline, C., (2023). Magnetotelluric monitoring of The Geysers geothermal field, northern California: Phase 2, *48th Workshop on Geothermal Reservoir Engineering*, *SGP-TR-233,* Stanford, California.

Peacock, J. R., Earney, T. E., & Schermerhorn, W. (2020a). Magnetotelluric and gravity data from the Northwest Geysers, California. *U.S. Geological Survey data release*. https://doi.org/10.5066/P94D21UL.

Peacock, J. R., Earney, T. E., Mangan, M. T., Schermerhorn, W. D., Glen, J. M., Walters, M., & Hartline, C. (2020b). Geophysical characterization of the Northwest Geysers geothermal. *Journal of Volcanology and Geothermal Research, 399*, 106882. https://doi.org/10.1016/j.jvolgeores.2020.106882.

Peacock, J. R., Thiel, S., Reid, P., & Heinson, G. (2012). Magnetotelluric monitoring of a fluid injection: Example from an enhanced geothermal system. *Geophysical Research Letters, 39*. https://doi.org/10.1029/2012gl053080.

Stark, M. A., Box W. T., Jr., Beall, J. J., Goyal K. P., & Pingol, A. S. (2005). The Santa Rosa -- Geysers Recharge Project, Geysers Geothermal Field, California, USA, Proceedings World Geothermal Congress, Antalya, Turkey, 24-29 April 2005.

Um, E. S., Commer, M., & Newman, G. (2014). A strategy for coupled 3D imagin of large-scale seismic and electromagnetic data sets: application to subsalt imaging. *Geophysics, 79*, ID1-ID13. https://doi.org/10.1190/geo2013-0053.1.

Um, E. S., Commer, M., Gritto, R., Peacock, J. R., Alumbaugh D. L., Jarpe, S. P., Hartline, C., (2023). Cooperative joint inversion of magnetotelluric and microseismic data for imaging The Geysers geothermal field, California, USA, Geophysics, 88, 5, WB45-WB54. https://doi.org/10.1190/geo2022-0521.1.

U.S. Geological Survey, (2020). 3D Elevation Program 1-Meter Resolution Digital Elevation Model (published 20200606), accessed January 18, 2024 at URL https://www.usgs.gov/the-national-map-data-delivery.